Open Access Full Text Article

ORIGINAL RESEARCH

Exploring the Dynamics of Hemorrhagic Fever with Renal Syndrome Incidence in East China Through Seasonal Autoregressive Integrated Moving Average Models

Fuyan Shi,[1] Changlan Yu,[2]
Liping Yang,[3] Fangyou Li,[2]
Jiangtao Lun,[4] Wenfeng Gao,[5]
Yongyong Xu,[6] Yufei Xiao,[1]
Sravya B Shankara,[7]
Qingfeng Zheng,[8] Bo Zhang,[9]
Suzhen Wang[1]

[1]Department of Health Statistics, School of Public Health and Management, Weifang Medical University, Weifang, Shandong, People's Republic of China; [2]Anqiu City Center for Disease Control and Prevention, Anqiu, Shandong, People's Republic of China; [3]Health and Medical Center, Xijing Hospital, Air Force Military Medical University, Xi'an, Shannxi, People's Republic of China; [4]Anqiu Meteorological Bureau, Anqiu, Shandong, People's Republic of China; [5]Department of Immunology and Rheumatology, Affiliated Hospital of Weifang Medical University, Weifang, Shandong, People's Republic of China; [6]Department of Health Statistics, School of Military Preventive Medicine, Air Force Military Medical University, Xi'an, Shannxi, People's Republic of China; [7]Program in Health: Science, Society, and Policy, Brandeis University, Waltham, MA, USA; [8]Institute for Hospital Management of Tsinghua University, Tsinghua Campus, Shenzhen, People's Republic of China; [9]Department of Neurology and ICCTR Biostatistics and Research Design Center, Boston Children's Hospital and Harvard Medical School, Boston, MA, USA

Correspondence: Bo Zhang; Suzhen Wang
Email bo.zhang@childrens.harvard.edu; wangsz@wfmc.edu.cn

Objective: The purpose of this study was to explore the dynamics of incidence of hemorrhagic fever with renal syndrome (HFRS) from 2000 to 2017 in Anqiu City, a city located in East China, and find the potential factors leading to the incidence of HFRS.

Methods: Monthly reported cases of HFRS and climatic data from 2000 to 2017 in the city were obtained. Seasonal autoregressive integrated moving average (SARIMA) models were used to fit the HFRS incidence and predict the epidemic trend in Anqiu City. Univariate and multivariate generalized additive models were fit to identify and characterize the association between the HFRS incidence and meteorological factors during the study period.

Results: Statistical analysis results indicate that the annualized average incidence at the town level ranged from 1.68 to 6.31 per 100,000 population among 14 towns in the city, and the western towns exhibit high endemic levels during the study periods. With high validity, the optimal $SARIMA(0,1,1)(0,1,1)_{12}$ model may be used to predict the HFRS incidence. Multivariate generalized additive model (GAM) results show that the HFRS incidence increases as sunshine time and humidity increases and decreases as precipitation increases. In addition, the HFRS incidence is associated with temperature, precipitation, atmospheric pressure, and wind speed. Those are identified as the key climatic factors contributing to the transmission of HFRS.

Conclusion: This study provides evidence that the SARIMA models can be used to characterize the fluctuations in HFRS incidence. Our findings add to the knowledge of the role played by climate factors in HFRS transmission and can assist local health authorities in the development and refinement of a better strategy to prevent HFRS transmission.

Keywords: hemorrhagic fever with renal syndrome, meteorological factors, autoregressive integrated moving average model, generalized additive model, prediction

Introduction

Hemorrhagic fever with renal syndrome (HFRS) is an acute viral syndrome caused by infection with one variety of hantavirus. Hantaviruses are transmitted by rodents and can be exposed to humans through infected urine, droppings, or saliva. Patients with HFRS are mainly treated through supportive therapy, with the management of the patient's vitals and treatment of secondary infections. A decrease in illness and death from HFRS has been showed with the use of intravenous ribavirin, an antiviral drug. HFRS is a critical infectious disease in developing countries, with major epidemics erupting in eastern Asia.[1,2]

In mainland China, HFRS remains a serious public health problem, with approximately 20,000–50,000 human cases reported annually, approximately 90% of the total cases worldwide.[3,4] Currently, HFRS is endemic in 28 of the 31 provinces in mainland China, and the highest incidence was reported in the middle and eastern part of China. Shandong Province, a developed coastal province in East China, is one of the most severely affected provinces in China.[5,6] In order to effectively prevent the spread of HFRS, the Chinese Center for Disease Control and Prevention (CDC) established a surveillance system for HFRS in 2004 and created educational programs for the general public. It is challenging to eliminate HFRS completely because many factors, such as diverse animal reservoirs and climate factors, may influence the control effects.

Many studies have suggested that epidemic modelling and forecasting can be essential and effective tools to prevent and control HFRS.[7–9] The development and application of an HFRS incidence forecasting model are effective for improving the understanding of the epidemic characteristics of HFRS and can be helpful for the prevention and control of HFRS. Currently, statistical models used to predict the epidemics of HFRS include linear regression models,[10,11] negative binomial multivariable regression,[12] time series generalized additive models,[13] generalized linear models (GLMs),[14] autoregressive integrated moving average (ARIMA) models,[15,16] generalized additive models (GAMs),[17] and nonlinear autoregressive neural networks (NARNNs) and ARIMA-NARNN models.[8] Among those methods, the ARIMA models are the most common and useful method for modelling the temporal dependence structure of the time series of HFRS. The ARIMA models can take into account changing trends, periodic changes, and random disturbances in a time series. In epidemiology, ARIMA models have been successfully used to predict the incidence of tuberculosis,[18] dengue,[19] as well as other infectious diseases.[20]

Some studies predicted HFRS epidemics using ARIMA models and obtained a basis for targeted prevention and control measures.[15,16] These studies showed that ARIMA models had better predictive performance than other models. However, there was still inconsistency in how to use the ARIMA models and apply them to a particular region, making it difficult for researchers to choose the appropriate model to predict an HFRS epidemic. This inconsistency may be due to the fact that there are many influencing factors, such as immunization, temperature, humidity,

elevation, and the local rat species.[1,3,21,22] This prevents the HFRS prediction model constructed from a particular region from being universal. As a result, a specific prediction model based on the actual data of the region needs to be constructed to predict the epidemics of HFRS in a region accurately.

Previous studies indicated that some areas in China were moderate endemic areas with HFRS incidences between 5.0 and 30.0 per 100,000 population from 1994 to 1998.[16–18,20,21] However, few studies explored the dynamics of HFRS incidence and investigated the potential factors leading to this disease.[23] In the present study, the key climatic drivers of HFRS transmission were identified by the GAMs, a descriptive analysis of HFRS with a spatiotemporal distribution was explored, and the optimal seasonal ARIMA (SARIMA) model for predicting HFRS incidences was developed for Anqiu City, a major administrative region in Shandong Providence in East China. The results of this study can help predict the future trends of HFRS to prevent and control HFRS more accurately.

Methods
Study Data
The study area is the Anqiu City in Shandong Province, the middle of the Shandong Peninsula. This city has a warm temperate continental climate influenced by the monsoon, with an annual mean temperature of 53.96°F and an average annual rainfall of 25.45 inches. Consisting of 14 towns, the study area's total population is 0.95 million, among which farmers account for 0.78 million. The main crops of the study area are wheat, corn, and peanut, and most farmers reside less than 55 yards from their farmlands. As traditional farming methods provide an opportunity for wild rodent propagation, suitable living conditions and sufficient food resources are created, which allow for an increase in transmission of HFRS between rodents and from rodents to humans.

The monthly HFRS cases recorded in the study area from 2000 to 2017 were collected from the City Center for Disease Control and Prevention (CDC). The National Infectious Disease Reporting system reported all HFRS cases to the City CDC, which verified all the HFRS cases that were first diagnosed in hospitals or clinics. The city's population data from 2000 to 2017 were determined based on information from the City Bureau of Statistics. Environmental factors for the city during the

study periods, including monthly average temperature, average air pressure, average sunshine, average wind speed, monthly precipitation, and average moisture, were collected from the City Meteorological Bureau. Over the course of the 18-year study period, 794 cases were registered in the study area.

Statistical Analysis

The ARIMA models are one of the most commonly applied time series prediction models,[24] using the hybrid modelling approach of autoregressive (AR) and moving average (MA) methods. ARIMA models have abilities to represent a non-seasonal time series and be used to produce an accurate forecast based on the historical data of a single variable. It is usually expressed as $ARIMA(p,d,q)$, where p is the number of AR lags, q is the number of MA lags, and d is the number of different passes. ARIMA models are also capable of modelling a wide range of seasonal data. Seasonality in a time series refers to a seasonal pattern of changes that repeats over s time periods (s is the number of time periods until the pattern repeats again). In a seasonal ARIMA (SARIMA) model, seasonal AR and MA terms predict the time series using data values and errors at times with lags that are multiples of s.[24] In a SARIMA model, the time series Y_t is assumed to be generated by a $SARIMA(p,d,q)(P,D,Q)s$ process with mean μ of the Box-Jenkins's model[24] if

$$\varphi(B)\phi(B^s)(1-B)^d(1-B^s)^D(Y_t-\mu) = \theta(B)\Theta(B^s)a_t,$$

where

$$\varphi(B) = 1 - \varphi_1 B - \varphi_2 B^2 - \ldots - \varphi_p B^p$$

$$\phi(B^s) = 1 - \phi_1 B^s - \phi_2 B^{2s} - \ldots - \phi_P B^{Ps},$$

and

$$\Theta(B^s) = 1 - \Theta_1 B^s - \Theta_2 B^{2s} - \ldots - \Theta_Q B^{Qs}.$$

Here, p is the number of AR lags, q is the number of MA lags, and d is the number of regular differences, and the seasonal parameters include seasonal AR lags, seasonal MA lags Q, seasonal differences D, and the length of the seasonal periods or periodicity s.[25] In a SARIMA model, B is backward shift operator and others are unknown parameters. The SARIMA model formulation includes four steps: identifying the $SARIMA(p,d,q)(P,D,Q)s$ structure, estimating unknown parameters, performing goodness-of-fit tests on the estimated residuals, and predicting future outcomes.

In this study, the augmented Dickey-Fuller Unit Root (ADF) test was applied to estimate the stationarity of the time series.[26,27] If the time series is not stationary, an appropriate difference can be used to make the series stationary. The Box and Jenkins method was used to construct the SARIMA model in this study.[28] The autocorrelation functions (ACF) and partial autocorrelation functions (PACF) of the transformed data were utilized to determine the seasonal and non-seasonal orders and identify an appropriate SARIMA model. The conditional least squares method was applied to estimate the model parameters. In model diagnosis, white-noise test methods were employed to check whether the residuals were independent and normally distributed.[29] Several models can be constructed, and the selection of an optimal SARIMA model is necessary. The model selection was conducted based on normalized Bayesian information criterion (BIC) and Ljung-Box Q test. In addition, coefficient of determination (R^2), root-mean-square error (RMSE), mean absolute error (MAE), and maximum absolute error (MaxAE) were selected as the measures to evaluate the SARIMA models.[24]

Univariate and multivariate generalized additive models (GAMs) with a logarithm link assuming that the HFRS incidence conditionally follows a Poisson distribution were fit to determine on how the meteorological factors affect the monthly HFRS incidence. The meteorological factors utilized in this study included monthly average temperature, precipitation, sunshine time, humidity, atmospheric pressure, and wind speed. Spatial distribution maps were created for the study area across the 18-year study period. All of these analyses were conducted by statistical software SPSS (Version 17.0, SPSS, Chicago, Illinois, USA) and R (Version 3.6.1, R Core Team, Vienna, Austria). This study conformed to the provisions of the Declaration of Helsinki and was approved by the Ethics Committee of Weifang Medical University (No. 2019SL059). The data in this study were accessed from the Anqiu City Center for Disease Control and Prevention and are freely available upon request.

Results

Descriptive Analysis

A total of 794 cases were registered in the study area during the 18-year period. The highest average incidence rate was 15.05 per 100,000 population in 2000, and the lowest average incidence rate was 1.15 per 100,000 population in 2006, with an annual incidence rate of 4.36 per

100,000 population. Among the total cases, 69.50% were male, and 30.50% were female, with a gender ratio (male vs female) of 2.28. Among those patients, about 1.26% were children under 15 years old, 7.05% were older adults over the age of 64 years, and others were between 15 and 64 years of age. Regarding occupation, 1.01% were outdoor workers that include migrant workers and construction workers, 5.67% were students, and farmers accounted for 83.00%. The monthly HFRS cases for the 18 years from 2000 to 2017 are shown in Figure 1, which indicates that the incidence of HFRS presented apparent seasonal character. There were two high peaks every year, the smaller epidemic peak occurred in spring between March and April, and the larger peak occurred in late fall and early winter between October and November.

To visualize the spatial and temporal variations in the HFRS incidence rates in the study area across the 18-year study period, the annualized average incidence of HFRS per 100,000 population was calculated for each town in the City over the 18-year period. Then, the annualized average incidences for each town were mapped in gradient colors in spatial distributions maps (Figure 2). Figure 2(A-R) show that the annual incidence of HFRS gradually decreased from 2000 to 2006, and the lowest incidence of 1.15 cases per 100,000 population occurred in 2006. Since 2007, the annual incidence of HFRS has increased gradually. Figure 2(S) shows the annualized average incidence for 14 towns within the City from 2000 to 2017. The annual average incidence at the town level ranged from 1.68 to 6.31 per 100 000 population.

Analysis Results from the SARIMA Models

Monthly data of HFRS from 2000 to 2016 were used as the training data set for fitting the SARIMA models, and those for 2017 were used as the test data set. Figure 1 shows that the onset of HFRS has seasonal characteristics with a seasonal cycle every 12 months and there was a non-stationary trend. Therefore, a first-order trend difference and a first-order seasonal difference were used to stabilize the average HFRS incidence. The ADF test result showed that the converted series improved stability after first-order difference (Dickey-Fuller $= -5.071$, p-value $= 0.010$). The diagnostic plots of ACF and PACF for original time series, first-order difference series, and residuals of the $ARIMA(2, 1, 1)$ model were created in Figure 3. Figure 3 suggests that the $ARIMA(2, 1, 1)$ model is sufficient to explain the information of the monthly

HFRS time series. Therefore, to fit the SARIMA models with a maximum order of 2 in the AR terms, a maximum order of 1 in the MA terms, and a first-order difference, we created seven candidate models: $SARIMA(0, 1, 1)(0, 1, 1)_{12}$, $SARIMA(0, 1, 2)(0, 1, 2)_{12}$, $SARIMA(1, 1, 0)(1, 1, 0)_{12}$, $SARIMA(1, 1, 1)(1, 1, 1)_{12}$, $SARIMA(1, 1, 2)(1, 1, 2)_{12}$, $SARIMA(2, 1, 0)(2, 1, 0)_{12}$, and $SARIMA(2, 1, 1)(2, 1, 1)_{12}$ (see Table 1). According to the parameter estimation and goodness of fit test results (see Tables 1 and 2), the $SARIMA (0, 1, 1)(0, 1, 1)_{12}$ model with the smallest normalized BIC was selected as the final model. The goodness-of-fit analysis indicated that there was no significant autocorrelation among residuals with different lags (Ljung-Box $Q = 19.551$, p-value $= 0.241$). The monthly data were taken to construct the $SARIMA(0, 1, 1)(0, 1, 1)_{12}$ model (see Table 3 and Figure 3), and the monthly data in 2017 were taken to test the model. The predicted data, actual data and the 95% confidence limit for the predicted data for 2017 are shown in Table 3 and Figure 3. The predicted numbers of HFRS cases match the observed, and the observed fell within the 95% confidence interval of the predicted incidence.

Analysis Results Given by the Generalized Additive Models

The univariate GAM was applied to separately analyze the influences of each meteorological factor on the monthly cases of HFRS. The results are reported in Table 4. The results show that all the six meteorological factors passed the significance test with a p-value less than 0.001, suggesting that each meteorological factor had a statistically significant impact on the monthly incidence of HFRS. The explained deviance of wind speed and temperature are high (20.1% and 12.5%, respectively). The corresponding adjusted coefficients of determination (adjusted R^2) were 0.244 and 0.064 for wind speed and temperature, respectively.

A multivariate GAM was fit to data, with the monthly cases of HFRS as the response variable and the meteorological factors, monthly average temperature, precipitation, sunshine time, humidity, atmospheric pressure, and wind speed, as the covariates. Table 5 reports the estimated effects from fitting the multivariate GAM, in terms of effective degrees of freedom (EDFs), reference degrees of freedom (RDFs), chi-square statistics, the corresponding p-values, explained deviance, and adjusted coefficients of determination. The analysis results indicate that the six
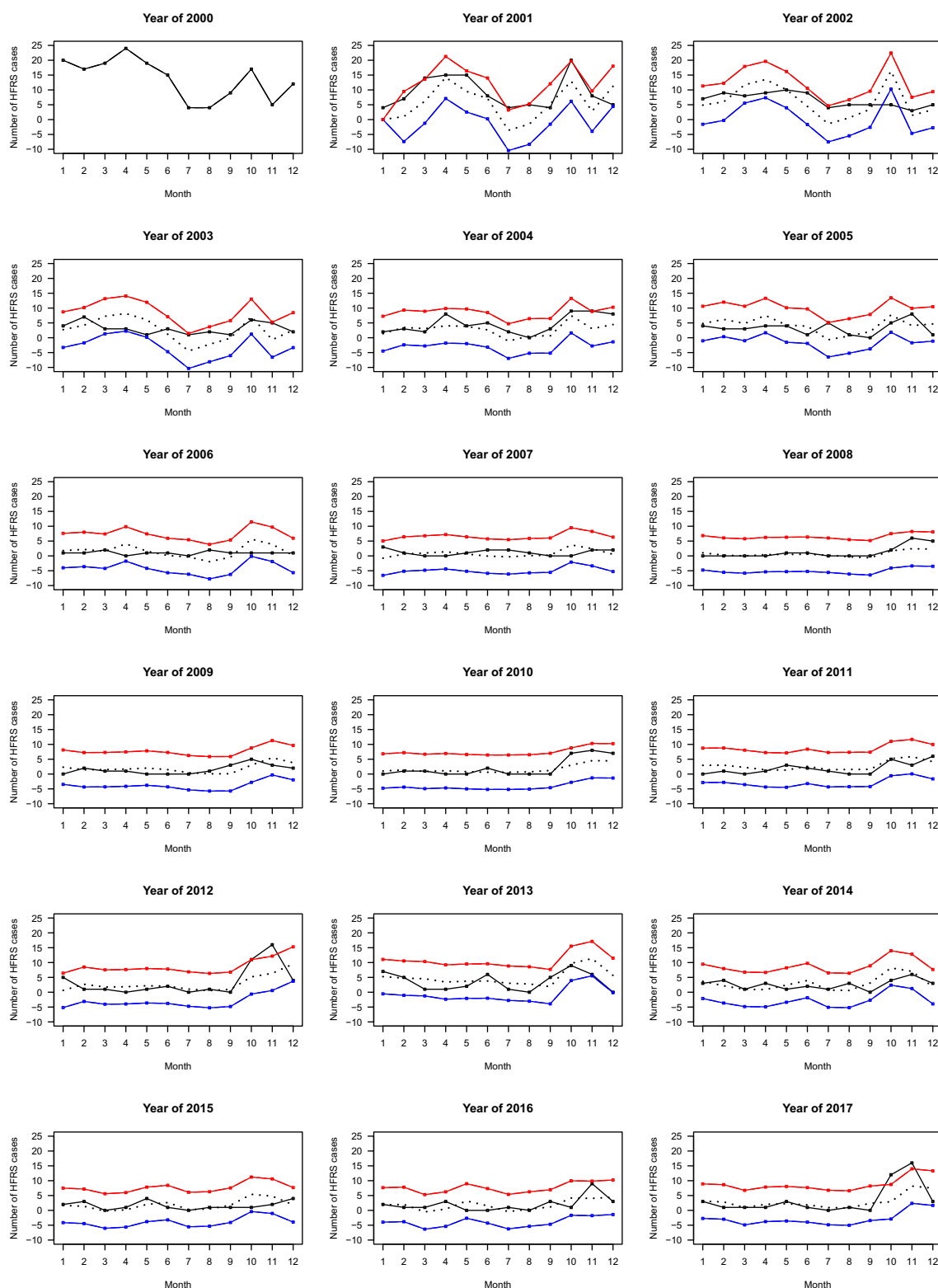
Figure 1 Observed (2000–2017), fitted (2001–2016), and predicted (2017) cases of hemorrhagic fever with renal syndrome (HFRS). Black solid line: observed cases; black dashed line: $SARIMA(0,1,1)(0,1,1)_{12}$ model fitted curve; red solid lines: upper bound of 95% confidence intervals for fitted values and 95% confidence limits for predicted values; blue solid lines: lower bound of 95% confidence intervals for fitted values and 95% confidence limits for predicted values.
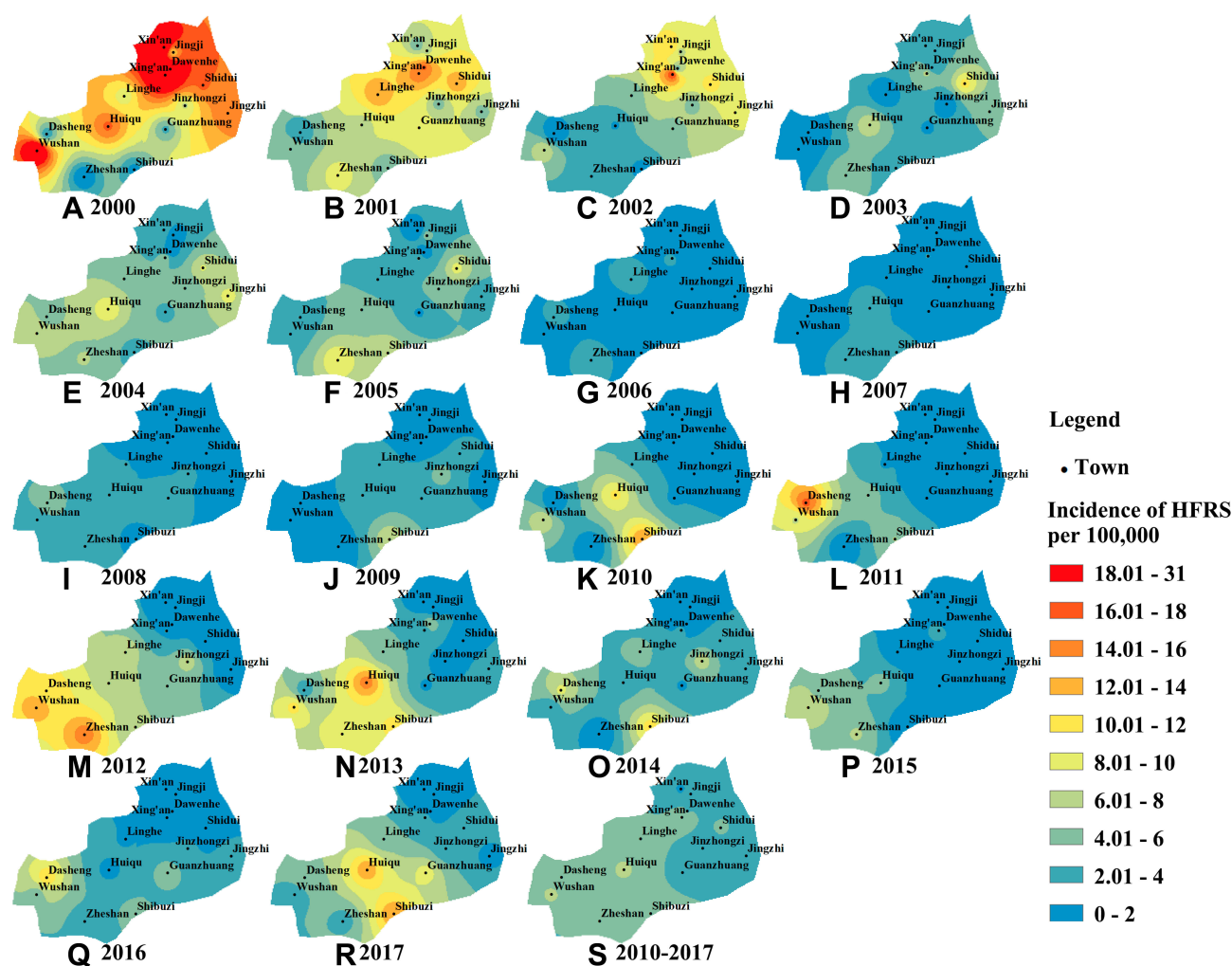
Figure 2 Spatial distribution of hemorrhagic fever with renal syndrome (HFRS) incidence per 100,000 population from 2000 to 2017 (Panel (**A**)–Panel (**R**)) and their average incidence (Panel (**S**)) in each town (each town is represented by a black dot with its name).

meteorological factors are statistically significant factors to influence the monthly HFRS incidence. Estimated smooth functions of six meteorological factors on monthly HFRS incidence are plotted in Figure 4. The fitted multivariate GAM had an explained deviance of 52.8% and an adjusted R^2 of 0.504. The reported EDFs show that sunshine time is linearly correlated with the HFRS incidence, but the other five meteorological factors are nonlinearly associated with the incidence with the EDFs that are much greater than one. These results also indicate that the HFRS incidence increases as sunshine time and humidity increase and decrease as precipitation increases. In addition, the HFRS incidence increases until wind speed increases to a peak at approximately 4.0 m/s (meters per second), and atmospheric pressure increases to a peak at approximately 1018 hPa (hectopascals), and then decreases.

Discussion

Our study showed that the incidence of HFRS presented apparent seasonality and that there were two annual peaks in Anqiu City in East China: the smaller peak occurred in spring between April and June, and the larger peak occurred in winter between October and November. Our results support the need to carry out deratization campaigns in spring and winter around the City as well as enhance population immunity by vaccination throughout the year. In addition, we applied a $SARIMA(0,1,1)(0,1,1)_{12}$ model to analyze the HFRS surveillance data. Based on the results above, the $SARIMA(0,1,1)(0,1,1)_{12}$ model is reliable with high prediction accuracy and can be used to predict the HFRS incidence in the City in the subsequent year. The prediction results suggested that the HFRS SARIMA model has a strong ability to forecast and predict the incidence of HFRS.
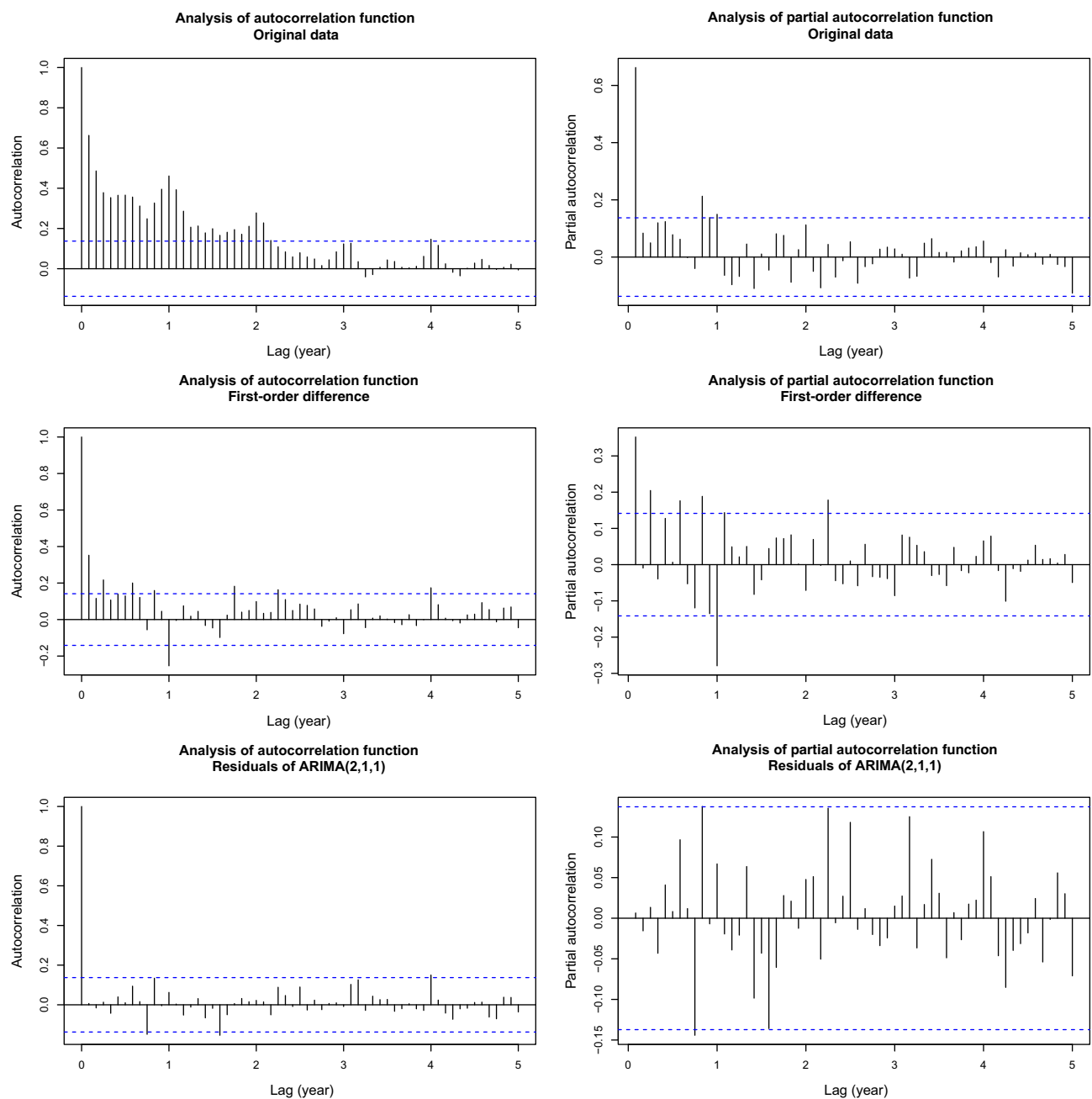
Figure 3 Analysis of autocorrelation and partial autocorrelation plots original time series, first-order difference series, and residuals of the $ARIMA(2, 1, 1)$ model of monthly cases of hemorrhagic fever with renal syndrome (HFRS).

Therefore, it is imperative and necessary to learn about the knowledge of HFRS forecasts, which can help health agencies to allocate health resources reasonably.

Our study also indicated that HFRS incidence was high from 2000 to 2002 and remained low until in 2012 (Figure 1). The slight rebound from 2012 may be triggered by the reconstruction and renovation of some areas of the City in recent years, which included the renovation of a large number of houses, destroyed the rodent habitat,

and made rats move frequently. These renovations also decreased the quality of the living environments of villagers and increased the chances of coming in contact with hantavirus, which further caused an increase in HFRS incidence. Based on our results, the government can allocate more health resources to high-risk areas and reduce the number of these resources used in low-risk areas to improve the effectiveness of interventions and the allocation of medical resources.

Table 1 Comparison of Candidate SARIMA Models

SARIMA Model	Goodness-of-Fit Statistics					Ljung-Box Q Test	
	R^2	RMSE	MAE	MaxAE	Normalized BIC	Statistic	p-value
$SARIMA(0,1,1)(0,1,1)_{12}$	0.230	3.001	2.232	11.134	2.280	19.551	0.241
$SARIMA(0,1,2)(0,1,2)_{12}$	0.255	2.968	2.159	10.526	2.313	16.964	0.258
$SARIMA(1,1,0)(1,1,0)_{12}$	0.046	3.341	2.536	12.873	2.495	47.655	0.000
$SARIMA(1,1,1)(1,1,1)_{12}$	0.251	2.977	2.173	10.629	2.319	17.998	0.207
$SARIMA(1,1,2)(1,1,2)_{12}$	0.265	2.964	2.176	10.201	2.365	16.303	0.178
$SARIMA(2,1,0)(2,1,0)_{12}$	0.167	3.138	2.413	13.478	2.425	30.855	0.006
$SARIMA(2,1,1)(2,1,1)_{12}$	0.257	2.980	2.170	10.271	2.376	16.425	0.173

Abbreviations: R^2, coefficient of determination; RMSE, root mean square error; MAE, mean absolute error; MaxAE, maximum absolute error; BIC, Bayesian information criterion.

Table 2 Parameter Estimation for the Selected $SARIMA(0,1,1)(0,1,1)_{12}$ model

Parameter	Estimate	Standard Error	t-Statistic	p-value
Constant	− 0.065	0.101	− 0.647	0.518
MA(1)	0.762	0.051	14.949	<0.001
SMA(12)	0.639	0.067	9.593	<0.001

Abbreviations: MA, moving average; SMA, seasonal moving average.

In our study, the GAMs were fit to further explore how the environmental factors affect HFRS incidence. The analysis results given by the GAMs support an irregular non-linear association between temperature and HFRS incidence. Yet, a previous study identified a negative association between temperature and HFRS incidence.[30] This may be due to the fact that high temperatures can limit the time available to farmers for outdoor activity and work,

Table 3 Comparison of Observed Cases and Predicted Cases of Hemorrhagic Fever with Renal Syndrome (HFRS) from January 2017 to December 2017

Month	Observed HFRS Cases	Predicted HFRS Cases	95% Confidence Interval	Residuals
January	3.00	3.09	(− 2.72, 8.91)	− 0.09
February	1.00	2.84	(− 2.97, 8.66)	− 1.84
March	1.00	0.93	(− 4.89, 6.74)	0.07
April	1.00	2.04	(− 3.77, 7.86)	− 1.04
May	3.00	2.24	(− 3.58, 8.05)	0.76
June	1.00	1.86	(− 3.96, 7.67)	− 0.86
July	0.00	0.96	(− 4.86, 6.77)	− 0.96
August	1.00	0.79	(− 5.03, 6.61)	0.21
September	0.00	2.40	(− 3.42, 8.21)	− 2.40
October	12.00	2.91	(− 2.90, 8.73)	9.09
November	16.00	8.18	(2.36, 13.99)	7.82
December	3.00	7.49	(1.68, 13.31)	− 4.49

Table 4 Univariate Generalized Additive Model Analysis of Meteorological Factors on Monthly Incidence of Hemorrhagic Fever with Renal Syndrome

Meteorological Factor	EDF	RDF	Chi-Square Statistic	p-value	Deviance Explained (%)	Adjusted R^2
Temperature	8.220	8.832	102.700	<0.001	12.500	0.064
Precipitation	1.000	1.001	70.340	<0.001	9.850	0.065
Sunshine time	8.473	8.923	61.910	<0.001	6.350	0.027
Humidity	8.399	8.894	50.930	<0.001	5.920	0.004
Atmospheric pressure	8.603	8.953	104.900	<0.001	11.900	0.065
Wind speed	6.012	7.172	250.100	<0.001	20.100	0.244

Abbreviations: EDF, effective degrees of freedom; RDF, reference degrees of freedom; Adjusted R^2, adjusted coefficients of determination.

Table 5 Multivariate Generalized Additive Model Analysis of Meteorological Factors on Monthly Incidence of Hemorrhagic Fever with Renal Syndrome

Meteorological Factor	EDF	RDF	Chi-Square Statistic	p-value
Temperature	8.552	8.925	39.540	<0.001
Precipitation	4.358	5.373	19.520	0.002
Sunshine time	1.000	1.001	23.630	<0.001
Humidity	4.819	5.863	68.590	<0.001
Atmospheric pressure	7.427	8.371	46.540	<0.001
Wind speed	6.457	7.571	125.970	<0.001

Abbreviations: EDF, effective degrees of freedom; RDF, reference degrees of freedom.

thereby reducing the opportunity for contact between people and field mice, one of the most common agricultural pests and a natural vector of hantavirus. Also, some studies have suggested that the breeding rate of rodents is highest at temperatures between 50 and 77°F, which are favorable conditions for outdoor activity and work.[30] However,

inconsistent findings have been reported in other studies that indicated a positive association between temperature and the incidence of HFRS.[28,31] These discrepancies may be due to different local conditions, such as different rodent compositions, hantavirus serotypes, environments, and climates in the study regions, and also due to the strong assumption on a linear association between temperature and the incidence of HFRS. Our data indicate that precipitation is negatively associated with the incidence of HFRS. This finding is consistent with the findings of two previous studies.[32,33] Abundant precipitation could harm rodents by destroying their habitats. Furthermore, frequent rainfall may decrease the likelihood of rodent-to-human contact, rodent-to-rodent contact, and virus transmission due to decreased rodent activity and reduced human exposure. However, several previous studies showed inconsistent findings on the positive association between precipitation and HFRS incidence.[34–36] There is no clear explanation for such differences, which may reflect the heterogeneity in local climate conditions. Further studies should be
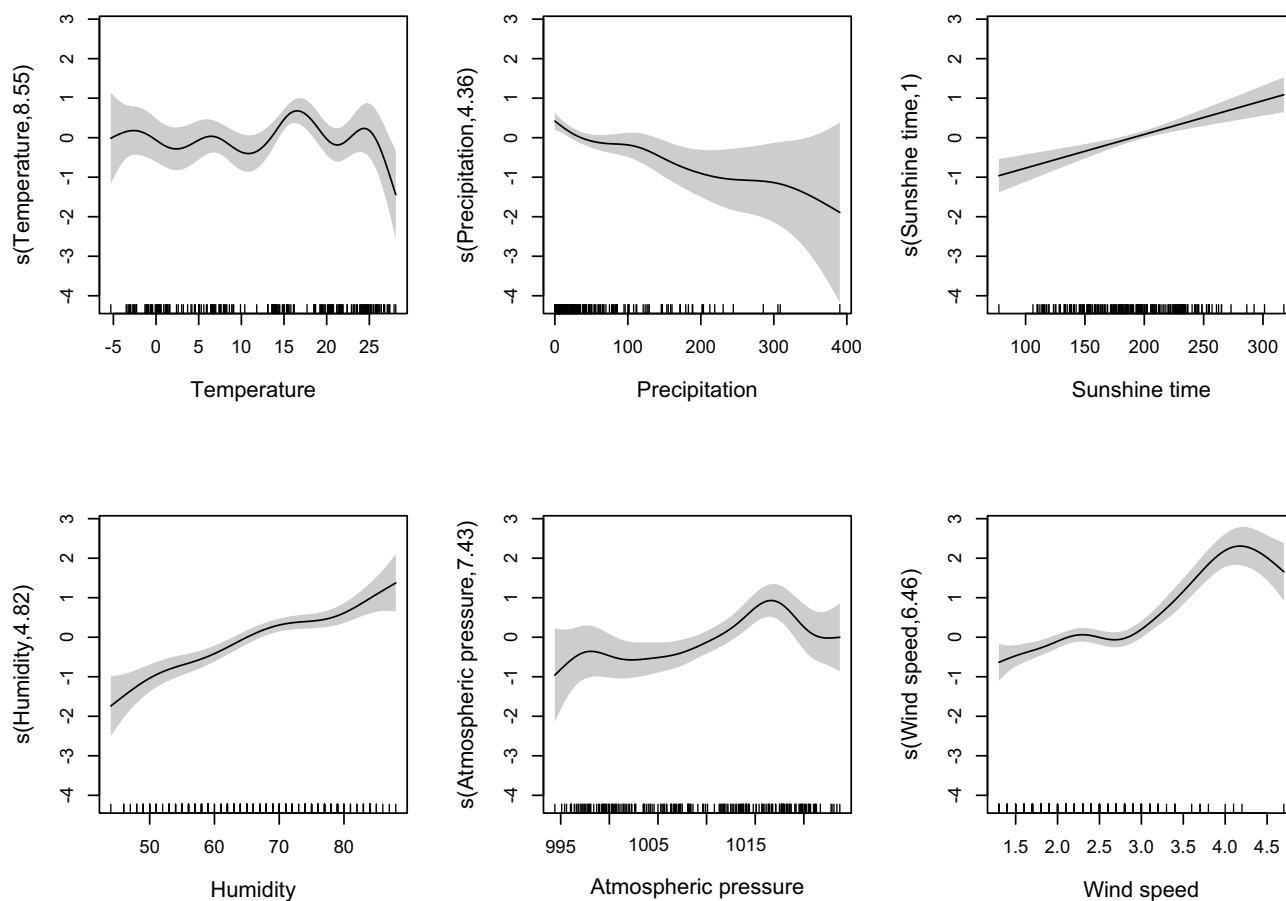

Figure 4 Estimated smooth functions of six meteorological factors on monthly incidence of hemorrhagic fever with renal syndrome (HFRS). Shaded areas represent 2 times standard errors above and below the estimate of the smooth functions.

conducted in different regions to gain a better understanding of the impact of precipitation on HFRS. The analysis results given by the GAMs show that sunshine time and humidity are positively associated with the monthly numbers of HFRS cases. In addition, the HFRS incidence increases until wind speed increases to a peak at approximately 4.0 m/s, and atmospheric pressure increases to a peak at approximately 1018 hPa, and then decreases. This is consistent with the results in a previous study.[37] Our investigation provides practical evidence for the usefulness of GAMs in HFRS prediction, with the optimum predictive climate variables being determined for different regions.

The SARIMA models with external covariates are named "SARIMAX" models. It is ideal to analyze the HFRS incidence using the SARIMAX models with flexible nonparametric representations of the covariates.[38] However, we found in the literature the developed SARIMAX models only include the external covariates in a parametric additive linear fashion, and such semiparametric SARIMAX models and their implementation procedures have not been developed.

Conclusions

Our study results can provide a quantitative basis for local disease control authorities to identify and potentially mitigate the risks associated with HFRS. This can be achieved by accurately predicting the fluctuation of HFRS with the SARIMA models and analysis approaches presented here. Such prediction can help improve the prevention and control of HFRS.[39]

Funding

Disclosure

References

1. Jonsson CB, Figueiredo LT, Vapalahti O. A global perspective on hantavirus ecology, epidemiology, and disease. *Clin Microbiol Rev.* 2010;23(2):412–441. doi:10.1128/CMR.00062-09
2. Vaheri A, Strandin T, Hepojoki J, et al. Uncovering the mysteries of hantavirus infections. *Nat Rev Microbiol.* 2013;11(8):539–550. doi:10.1038/nrmicro3066
3. Lei Yan L-QF, Hua-Guo H, Long-Qi Z, et al. Landscape elements and hantaan virus–related hemorrhagic fever with renal syndrome, People's Republic of China. *Emerg Infect Dis.* 2007;13(9):1301–1306. doi:10.3201/eid1309.061481
4. Shuo Zhang SW, Yin W, Liang M, et al. Epidemic characteristics of hemorrhagic fever with renal syndrome in China, 2006-2012. *BMC Infect Dis Vol.* 2014;14:384. doi:10.1186/1471-2334-14-384
5. Wang L, Wang T, Cui F, et al. Hemorrhagic fever with renal syndrome, Zibo City, China, 2006–2014. *Emerg Infect Dis.* 2016;22 (2):274–276. doi:10.3201/eid2202.151516
6. Wang T, Liu J, Zhou Y, et al. Prevalence of hemorrhagic fever with renal syndrome in Yiyuan County, China, 2005-2014. *BMC Infect Dis.* 2016;16:69. doi:10.1186/s12879-016-1404-7
7. Seung Seok Han SK, Choi Y, Kim S, Su Kim Y. Air pollution and hemorrhagic fever with renal syndrome in South Korea_ an ecological correlation study. *BMC Public Health.* 2013;13:347. doi:10.1186/ 1471-2458-13-347
8. Hualiang Lin ZZ, Liang L, Xiujun L, Liu Q. Meteorological factors are associated with hemorrhagic fever with renal syndrome in Jiaonan County, China, 2006–2011. *Int J Biometeorol.* 2014;58 (6):1031–1037. doi:10.1007/s00484-013-0688-1
9. Wu W, Guo J, An S, et al. Comparison of two hybrid models for forecasting the incidence of hemorrhagic fever with renal syndrome in Jiangsu Province, China. *PLoS One.* 2015;10(8):e0135492. doi:10.1371/journal.pone.0135492
10. Peng Bi XW, Fangzhen Zhang KA, Parton ST. Seasonal rainfall variability, the incidence of hemorrhagic fever with renal syndrome, and prediction of the disease in low-lying areas of China. *Am J Epidemiol.* 1998;148(3):276–281. doi:10.1093/oxfordjournals.aje.a009636
11. Olsson GE, Hjertqvist M, Lundkvist A, Hornfeldt B. Predicting high risk for human hantavirus infections, Sweden. *Emerg Infect Dis.* 2009;15(1):104–106. doi:10.3201/eid1501.080502
12. Wei Y, Wang Y, Li X, et al. Meteorological factors and risk of hemorrhagic fever with renal syndrome in Guangzhou, southern China, 2006-2015. *PLoS Negl Trop Dis.* 2018;12(6):e0006604. doi:10.1371/journal.pntd.0006604
13. Jiang F, Wang L, Wang S, et al. Meteorological factors affect the epidemiology of hemorrhagic fever with renal syndrome via altering the breeding and hantavirus-carrying states of rodents and mites: a 9 years' longitudinal study. *Emerg Microbes Infect.* 2017;6(11):e104. doi:10.1038/emi.2017.92

14. Wen-Yi Zhang W-DG, Fang L-Q, Chang-Ping L, et al. Climate variability and hemorrhagic fever with renal syndrome transmission in Northeastern China. *Environ Health Perspect*. 2010;118(7):915–920. doi:10.1289/ehp.0901504

15. Qiyong Liu XL, Jiang B, Yang W. Forecasting incidence of hemorrhagic fever with renal syndrome in China using ARIMA model. *BMC Infect Dis*. 2011;11:218. doi:10.1186/1471-2334-11-218

16. Wang T, Zhou Y, Wang L, Huang Z, Cui F, Zhai S. Using an autoregressive integrated moving average model to predict the incidence of hemorrhagic fever with renal syndrome in Zibo, China, 2004–2014. *Jpn J Infect Dis*. 2016;69(4):279–284. doi:10.7883/yoken.JJID.2014.567

17. Xiao DW, Tan K, Le X, Li J, Yan H, Xu Y. Modeling and predicting hemorrhagic fever with renal syndrome trends based on meteorological factors in Hu County, China. *PLoS One*. 2015;10(4):e0123166. doi:10.1371/journal.pone.0123166

18. Zheng YL, Zhang LP, Zhang XL, Wang K, Zheng YJ. Forecast model analysis for the morbidity of tuberculosis in Xinjiang, China. *PLoS One*. 2015;10(3):e0116832. doi:10.1371/journal.pone.0116832

19. Wongkoon S, Jaroensutasinee M, Jaroensutasinee K. Development of temporal modeling for prediction of dengue infection in Northeastern Thailand. *Asian Pac J Trop Med*. 2012;5(3):249–252. doi:10.1016/S1995-7645(12)60034-0

20. Liu L, Luan RS, Yin F, Zhu XP, Lu Q. Predicting the incidence of hand, foot and mouth disease in Sichuan province, China using the ARIMA model. *Epidemiol Infect*. 2016;144(1):144–151. doi:10.1017/S0950268815001144

21. Wen-Yi Zhang L-QF, Jiang J-F, Feng-Ming Hui GE, et al. Predicting the risk of hantavirus infection in Beijing, People's Republic of China. *Am J Trop Med Hyg*. 2009;80(4):678–683. doi:10.4269/ajtmh.2009.80.678

22. Xiang J, Hansen A, Liu Q, et al. Impact of meteorological factors on hemorrhagic fever with renal syndrome in 19 cities in China, 2005–2014. *Sci Total Environ*. 2018;636:1249–1256. doi:10.1016/j.scitotenv.2018.04.407

23. Fang LQ, Wang XJ, Liang S, et al. Spatiotemporal trends and climatic factors of hemorrhagic fever with renal syndrome epidemic in Shandong Province, China. *PLoS Negl Trop Dis*. 2010;4(8):e789. doi:10.1371/journal.pntd.0000789

24. Box GJ, Reinsel GC, Ljung GM. *Time Series Analysis: Forecasting and Control*. 2015.

25. Ho SL, X M, Goh TN. A comparative study of neural network and Box-Jenkins ARIMA modeling in time series prediction. *Comp Ind Eng*. 2002;42(2–4):371–375. doi:10.1016/S0360-8352(02)00036-0

26. Gerolimetto SM. On the power of the simulation-based ADF test in bounded time series. *Econ Bull*. 2017;37(1):539–552.

27. Galbraith JW, W VZ. On the distributions of Augmented Dickey–Fuller statistics in processes with moving average components. *J Econom*. 1999;93(1):25–47. doi:10.1016/S0304-4076(98)00097-9

28. Ljung GM, Box GEP. On a measure of lack of fit in time series models. *Biometrika*. 1978;65(2):297–334. doi:10.1093/biomet/65.2.297

29. Allard R. Use of time-series analysis in infectious disease surveillance. *Bull World Health Organ*. 1998;76(4):327–333.

30. Bai Y, Xu Z, Lu B, et al. Effects of climate and rodent factors on hemorrhagic fever with renal syndrome in Chongqing, China, 1997–2008. *PLoS One*. 2015;10(7):e0133218. doi:10.1371/journal.pone.0133218

31. Guan P, Huang D, He M, Shen T, Guo J, Zhou B. Investigating the effects of climatic variables and reservoir on the incidence of hemorrhagic fever with renal syndrome in Huludao City, China: a 17-year data analysis based on structure equation model. *BMC Infect Dis*. 2009;9:109. doi:10.1186/1471-2334-9-109

32. Bi P, Donald K, Parton K, Jinfa N. Climatic, reservoir and occupational variables and the transmission of haemorrhagic fever with renal syndrome in China. *Int J Epidemiol*. 2002;31(1):189–193. doi:10.1093/ije/31.1.189

33. Xiaodong Liu BJ, Weidong G, Liu Q. Temporal trend and climate factors of hemorrhagic fever with renal syndrome epidemic in Shenyang City, China. *BMC Infect Dis*. 2011;11:331. doi:10.1186/1471-2334-11-331

34. David M, Engelthaler DGM, Cheek JE, et al. Climatic and environmental patterns associated with hantavirus pulmonary syndrome, Four Corners region, United States. *Emerg Infect Dis*. 1999;5(1):87–94. doi:10.3201/eid0501.990110

35. Tamerius JD, Wise EK, Uejio CK, McCoy AL, Comrie AC. Climate and human health: synthesizing environmental complexity and uncertainty. *Stochastic Environ Res Risk Assess*. 2007;21(5):601–613. doi:10.1007/s00477-007-0142-1

36. Brian Hjelle GEG. Outbreak of hantavirus infection in the four corners region of the United States in the wake of the 1997-1998 El Nino-southern oscillation. *J Infect Dis*. 2000;181(5):1569–1573. doi:10.1086/315467

37. Tian H-Y, Yu P-B, Luis AD, et al. Changes in rodent abundance and weather conditions potentially drive hemorrhagic fever with renal syndrome outbreaks in Xi'an, China, 2005–2012. *PLoS Negl Trop Dis*. 2015;9(3):e0003530. doi:10.1371/journal.pntd.0003530

38. Duan Y, Huang XL, Wang YJ, et al. Impact of meteorological changes on the incidence of scarlet fever in Hefei City, China. *Int J Biometeorol*. 2016;60(10):1543–1550. doi:10.1007/s00484-016-1145-8

39. Puca EQM, Pipero P, Akshija I, Kote M, Kraja D. Two cases of imported hemorrhagic fever with renal syndrome and systematic review of literature. *Travel Med Infect Dis*. 2019;28:86–90. doi:10.1016/j.tmaid.2018.07.010